

Improving Intergranular Corrosion Resistance of Sensitized Type 316 Austenitic Stainless Steel by Laser Surface Melting

U.K. Mudali and R.K. Dayal

An attempt was made to modify the surface microstructure of a sensitized austenitic stainless steel, without affecting the bulk properties, using laser surface melting techniques. AISI type 316 stainless steel specimens sensitized at 923 K for 20 hr were laser surface melted using a pulsed ruby laser at 6 J energy. Two successive pulses were given to ensure uniform melting and homogenization. The melted layers were characterized by small angle X-ray diffraction and scanning electron microscopy. Intergranular corrosion tests were carried out on the melted region as per ASTM A262 practice A (etch test) and electrochemical potentiokinetic reactivation test. The results indicated an improvement in the intergranular corrosion resistance after laser surface melting. The results are explained on the basis of homogeneous and nonsensitized microstructure obtained at the surface after laser surface melting. It is concluded that laser surface melting can be used as an *in situ* method to increase the life of a sensitized component by modifying the surface microstructure.

1. Introduction

AUSTENITIC stainless steels are prone to intergranular corrosion (IGC) and intergranular stress-corrosion cracking (IGSCC) when they are subjected to sensitizing heat treatments between 723 and 1073 K, leading to premature failure of components during service. The sensitization is attributed to the formation of a chromium-depleted zone adjacent to the chromium-rich $M_{23}C_6$ carbides along the grain boundaries during the heat treatment. Thus, the presence of this heterogeneous microstructure can initiate IGC and IGSCC. To avoid this type of failure, the remedial methods include use of low-carbon stainless steels, high-temperature solution annealing treatment to dissolve the carbides, and use of carbide stabilizing alloy additions such as Ti and Nb.[1-3] However, if the components are found to be sensitized during the final stage of commissioning or during service, they cannot be used in hostile environments without solution annealing treatment. Also, it is difficult to eliminate a sensitized microstructure, such as the one formed at the heat-affected zones during welding, by a simple heat treatment without affecting the properties of the weldment. In such cases, an *in situ* method is required that can selectively eliminate the sensitized microstructure.

In the present work, an attempt was made to homogenize the surface of the sensitized specimens by using a laser. This would eliminate the possible initiation of IGC and IGSCC at the surface, because most corrosion processes initiate from the surface. It is known that laser surface modification produces microstructures with improved properties for many applications.[4-10] Also, laser surface melting can be carried out on complicated or inaccessible components *in situ* if required.[5] With careful beam control, appropriate melt depths can be produced, with minimum surface residual stresses and complete intermixing of the alloying components. Because melting during laser processing occurs in a very short time, and only in the surface region, the bulk of the material remains cool, thus serving as an infinite heat sink. Large temperature gradients exist across the boundary between the melted surface layer and the underlying solid substrate. This produces rapid self-quenching and resolidification, with quench rates as large as 10^{11} K sec^{-1} and accompanying resolidification velocities in the range of 20 ms^{-1}. The rapid quenching from the liquid phase can produce extended solid solutions, metastable crystalline phases, and, in some instances, metallic glasses.

In the present work, laser surface melting of sensitized type 316 stainless steel was carried out using a pulsed ruby laser system. The melted regions were characterized by using scanning electron microscopy (SEM) and X-ray diffraction (XRD). Intergranular corrosion resistance was evaluated by testing as per ASTM A262 practice A (etch test) and by conducting electrochemical potentiokinetic reactivation (EPR) tests.

2. Experimental Methods

Nuclear-grade type 316 stainless steel (see material in Table 1 for composition) was used for the present work. Solution annealed type 316 stainless steel was given a sensitization heat treatment at 923 K for 20 hr. Specimens of 10 by 10 by 2 mm were cut from this material and polished with up to 600-grade SiC emery paper. This surface preparation was preferred to minimize the reflection of the laser beam during melting. The specimens were thoroughly cleaned in methanol prior to laser surface melting. Laser surface melting was carried out using a pulsed ruby laser system (JK Industries, UK) with the following specifications: pulse width, 30 ns; λ, 693.4 nm; energy range, 1 to 10 J/pulse; and pulse frequency rate, 6 pulses per minute. In the present work, laser irradiation was carried out at a calibrated energy of 6 J per pulse with two successive pulses at the same spot. The diameter of the melted region, corresponding to the diameter of the laser beam, was about 6 mm. Complete melting of the surface was ensured by immediately

U.K. Mudali and **R.K. Dayal**, Metallurgy Division, Indira Gandhi Centre for Atomic Research, Kalpakkam, India.

Table 1 Chemical Composition of Type 316 Stainless Steel

Composition, wt.%									
C	N	Cr	Mo	Ni	Mn	Si	S	P	Fe
0.054	0.038	16.46	2.28	10.2	1.69	0.64	0.006	0.025	bal

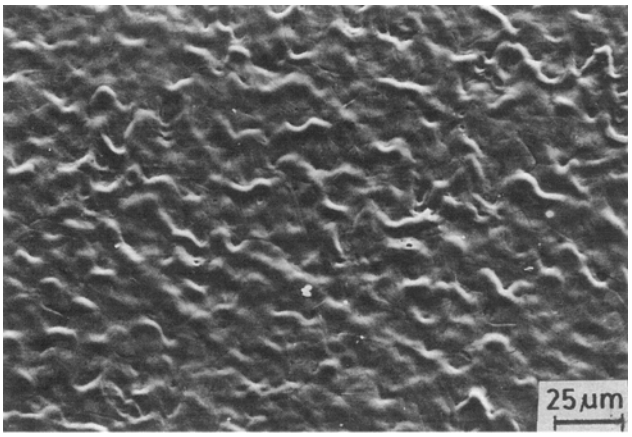

Fig. 1 Scanning electron micrographs of as-laser melted surface showing the presence of **(a)** ripples and craters on the surface and **(b)** striations and flow lines on the surface.

observing the melted samples in a low-power optical microscope and by visual observation. In some cases, an optical homogenizer was used as a wave guide to homogenize the beam energy for uniform and homogeneous melting throughout the region.

The melted regions were observed by SEM to examine the changes in the surface morphology. To determine the formation of any new phases during melting and solidification, small angle X-ray diffraction of the melted layer was carried out using a Rigaku model microprocessor-based X-ray diffractometer. Intergranular corrosion testing of the samples was carried out by electrolytically etching the samples in a 10% ammonium persulfate solution at 6 V for 90 sec.[11] The etched samples were observed in an optical microscope to classify the microstructure obtained. The EPR tests were carried out as per the procedures formulated by Clarke *et al.*[12] The test variables were as follows: electrolyte, $0.5M$ $H_2SO_4 + 0.01M$ NH_4SCN; scan rate, 6 V/hr; passivation potential and time, +200 mV (saturated calomel electrode) and 120 sec; deaeration by argon purging. According to this test, sensitized material exhibits a significant reactivation peak current and charge density values that can be related to the degree of sensitization. The higher the reactivation peak current and charge density values, the higher the degree of material sensitization. The superiority of this test over others is the selective attack on the chromium-depleted regions that contribute to intergranular corrosion. After electrolytic etching and EPR testing, the samples were examined by SEM.

3. Results and Discussion

Figure 1(a) shows the appearance of the surface of the laser surface melted samples as observed in SEM. The resolidified surface was rough in appearance, and a large number of craters and ripples were observed with a continuous wavy pattern. The occurrence of the craters and ripples was attributed to surface tension gradients and fluid flow effects produced during melting and resolidification.[13] At higher magnifications (Fig. 1b), striations or flow lines were found on the surface, which could be attributed to the quenching stresses created during the rapid heating and resolidification.[14] However, no microcracks or micropores were observed throughout the surface.

Figure 2(a) shows the structure obtained after electrolytic etching of a sensitized 316 stainless steel (923 K/20 hr) specimen. Complete attack of the grain boundaries in a continuous network is evident. This type of structure is called a "ditch" (according to the ASTM classification[11]) and indicates susceptibility to IGC or IGSCC during service. However, the laser surface melting samples did not show continuous grain boundary attack, as shown in Fig. 2(b).

The elimination of the ditch structure indicated an improvement in the intergranular corrosion resistance. Indeed, the center of the laser-melted zone clearly showed total elimination of the grain boundary attack, as shown in Fig. 3(a). Also, the redistribution of the grain boundary carbides into globular particles was observed at the interface between the melt zone and the unaffected base metal (Fig. 3b). This indicates incomplete melting and dissolution of the carbide particles in these areas.

However, the uniform distribution of such fine carbides has been reported to improve localized corrosion resistance.[15] It is also reported that a new surface can be created by laser surface melting, with total redistribution of the second phases, having improved properties.[6] The modification of the surface by laser surface melting eliminated the earlier microstructure, which provided a continuous pathway for IGC or IGSCC. Thus, a surface that has a nonsensitized microstructure is produced, although the bulk of the material may remain sensitized. Such an

improvement in IGC was reported by de Damborena *et al.* when they studied laser-modified sensitized 304 stainless steel using a continuous CO_2 laser.[16] They have attributed the improvement in IGC to the rapid solidification process, which produced a microstructure consisting of dendritic cellular growth of austenite. Similar improvement in IGC of sensitized 304 stainless steel was reported by Anthony and Cline[4] when they studied continuous wave CO_2 laser-melted samples by the Strauss test.

X-ray diffraction results of the samples showed a decrease in the intensity and broadening of the austenite (gamma phase) peaks, with an increase in the full width at half maximum (FWHM) compared to the as-sensitized samples. However, there was not much shift in the *d*-spacing values after laser surface melting. The broadening of the peaks could be attributed to the presence of quenching stresses or the formation of a near-

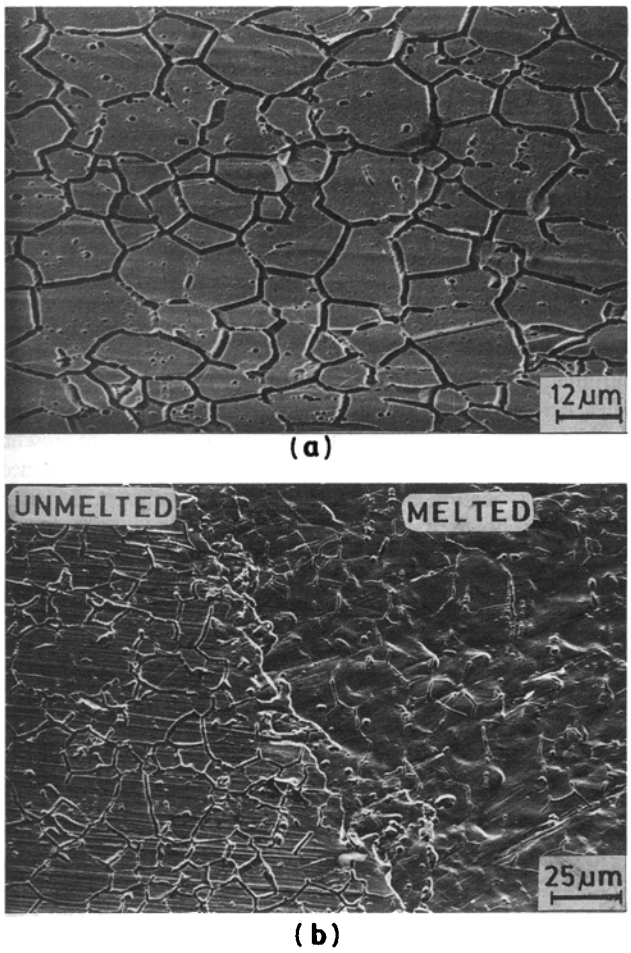

Fig. 2 Scanning electron micrographs after etch testing showing **(a)** as-sensitized microstructure and **(b)** reduction in the continuous network of grain boundaries after laser surface melting.

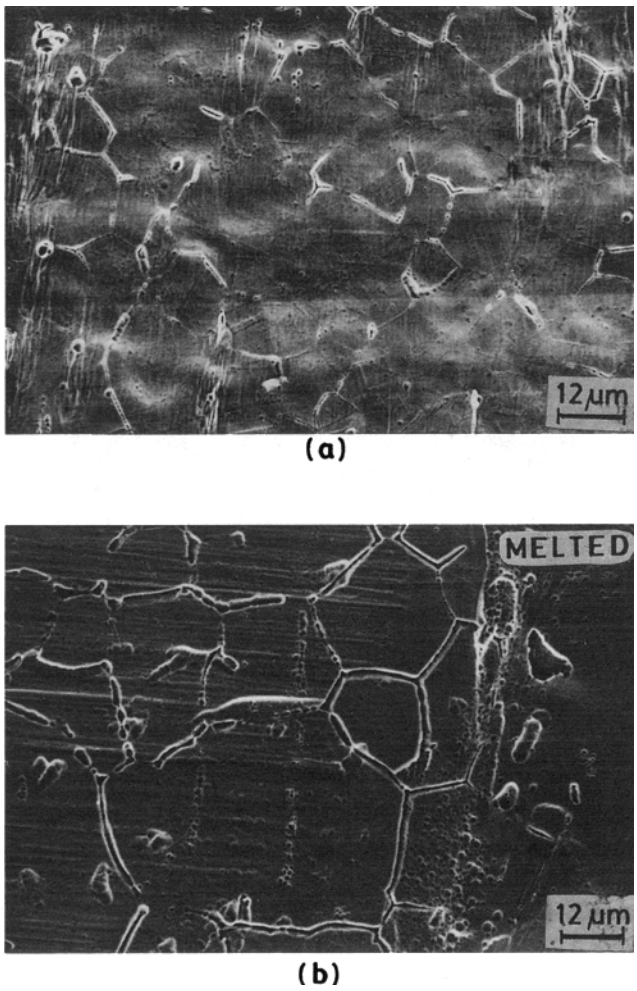

Fig. 3 Scanning electron micrographs of test samples showing **(a)** the complete disappearance of grain boundary network and the presence of residual carbide particles and **(b)** the carbide particles present between the melt zone and the unaffected base metal.

Table 2 XRD Data for Type 316 Stainless Steel

Condition	2è, degree	FWHM, in.	*d*, A°	I/Io	Plane
Sensitized at 923 K for 20 hr	44.34	0.980	2.041	100	(111)
	51.6	0.660	1.770	25	(200)
	75.94	0.660	1.252	13	(220)
Sensitized and laser surface melted	44.42	1.080	2.038	99	(111)
	51.64	0.750	1.769	46	(200)
	75.92	0.810	1.252	26	(220)

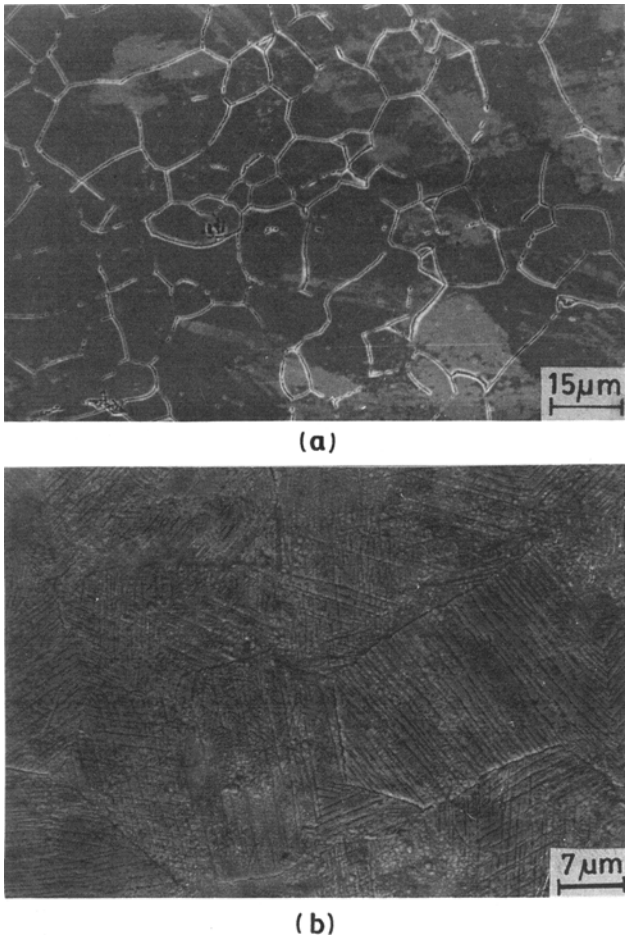

Fig. 4 Scanning electron micrographs of the EPR tested samples showing (**a**) continuous network of grain boundary attack for as-sensitized samples and (**b**) no selective grain boundary attack for laser surface melted samples.

amorphous or microcrystalline structure developed after laser surface melting.[7,17] This was also confirmed by the presence of striations or flow lines observed in the SEM photomicrographs of the samples (Fig. 1b). The results of the XRD analysis are given in Table 2.

The SEM observation (Fig. 4) of the samples after EPR testing showed the continuous attack of grain boundaries for the as-sensitized samples, whereas no grain boundary attack was revealed for the laser surface melted samples. However, striations and flow lines were clearly visible.

The EPR tests showed less significant reactivation peak for the laser surface melted samples compared to the as-sensitized samples (Fig. 5). The reactivation peak current density (15.8 mA/cm^2) and the EPR charge values (1.03 C/cm^2) were quite high for the as-sensitized samples. This clearly indicated the formation of a microstructure without any significant chromium depletion after laser surface melting. Also, this confirmed the total redistribution of the carbides, with no detectable chromium-depleted region.

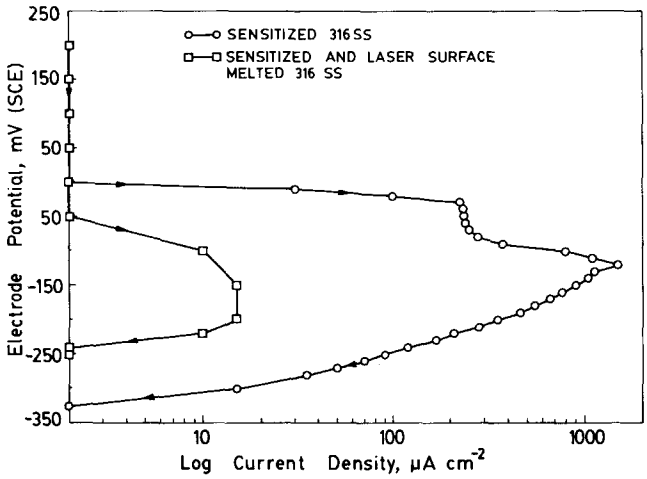

Fig. 5 EPR curves of sensitized, as well as sensitized and laser surface melted, specimens.

4. Conclusions

Laser surface melting can modify the microstructure by eliminating sensitization at the surface of type 316 stainless steel. No micropores or microcracks were observed after laser surface melting; however, striations or flow lines were present, and this could be attributed to the quenching stresses formed due to rapid heating and resolidification. Significant reduction of the grain boundary carbide network, with the redistribution of carbides into globular particles, was observed after laser surface melting. Laser surface melting of sensitized type 316 stainless steel improved the intergranular corrosion resistance without affecting the bulk properties.

Acknowledgment

The authors thank Shri J.B. Gnanamoorthy, Head, Metallurgy Division, and Dr. Placid Rodriguez, Head, Metallurgy and Materials Programme, for their keen interest in the work. Also, thanks are due to Prof. Dr. S.B. Ogale and Dr. S.M. Kanetkar of the University for their help and for the use of their laser system, and Mrs. M. Radhika for help in SEM observation of the samples.

References

1. R.L. Cowan, II and C.S. Tedmon, Jr., *Advances in Corrosion Science and Technology*, Vol 3, M.G. Fontana and R.W. Staehle, Ed., Plenum Press, New York, 293-400 (1973).
2. V. Cihal, *Intergranular Corrosion of Steels and Alloys*, Elsevier Publishing, Amsterdam (1984).
3. F.G. Wilson, *Brit. Corrosion J., 6*, 100-187 (1971).
4. T.R. Anthony and H.E. Cline, *J. Appl. Phys., 49*, 1248 (1978).
5. M. Bass, Ed., *Laser Materials Processing: Materials Processing—Theory and Practice*, vol 3, North Holland Publishing, Amsterdam (1983).

6. K. Mukherjee and J. Mazumder, *Lasers in Metallurgy,* Metallurgical Society of AIME, New York (1981).
7. C.W. Draper and J.M. Poate, *Int. Met. Rev., 30,* 85-108 (1985).
8. E.I. Meletis and R.F. Hochman, *J. Met., 39,* 25-27 (1987).
9. D.S. Gnanamuthu, *Applications of Lasers in Materials Processing,* E.A. Metzbower, Ed., American Society for Metals, 177 (1979).
10. W.M. Steen, Proceedings of Second European Conference on Laser Treatment of Materials, Bad Nauheim, 60-64 (1988).
11. "Standard Recommended Practices for Detecting Susceptibility to Intergranular Attack in Stainless Steels," ASTM A 262 Practice A, Vol 03.02, American Society for Testing and Materials, Philadelphia, 2 (1986).
12. W.L. Clarke, R.L. Cowan, and W.L. Walker, "Intergranular Corrosion of Stainless Alloys," ASTM STP 656, American Society for Testing and Materials, Philadelphia, 99-132 (1978).
13. T.R. Anthony and H.E. Cline, *J. Appl. Phys., 48,* 3888 (1977).
14. M. Lamb, W.M. Steen, and D.R.F. West, Proceedings of International Conference on Stainless Steel 84, Gothernburg, Sweden, 295-302 (1984).
15. T. Tsuru and R.M. Latanision, *Corrosion and Corrosion Protection,* R.P. Frankenthal and F. Mansfeld, Ed., The Electrochemical Society, Pennington, 238 (1981).
16. J. de Damborena, A.J. Vazquez, J.A. Gonzalez, and D.R.F. West, *Surface Engineering, 5,* 235 (1989).
17. B.D. Cullity, *Elements of X-ray Diffraction,* 2nd ed., Addison-Wesley, New York (1978).